



HAL
open science

Numerical study of the stabilization of 1D locally coupled wave equations.

Stéphane Gerbi, Chiraz Kassem, Amina Mortada, Ali Wehbe

► **To cite this version:**

Stéphane Gerbi, Chiraz Kassem, Amina Mortada, Ali Wehbe. Numerical study of the stabilization of 1D locally coupled wave equations.. 2020. hal-03099299

HAL Id: hal-03099299

<https://hal.science/hal-03099299>

Preprint submitted on 6 Jan 2021

HAL is a multi-disciplinary open access archive for the deposit and dissemination of scientific research documents, whether they are published or not. The documents may come from teaching and research institutions in France or abroad, or from public or private research centers.

L'archive ouverte pluridisciplinaire **HAL**, est destinée au dépôt et à la diffusion de documents scientifiques de niveau recherche, publiés ou non, émanant des établissements d'enseignement et de recherche français ou étrangers, des laboratoires publics ou privés.

NUMERICAL STUDY OF THE STABILIZATION OF 1D LOCALLY COUPLED WAVE EQUATIONS.

STÉPHANE GERBI, CHIRAZ KASSEM, AMINA MORTADA, AND ALI WEHBE

ABSTRACT. In this paper, we study the numerical stabilization of a 1D system of two wave equations coupled by velocities with an internal, local control acting on only one equation. In the theoretical part of this study [3], we distinguished two cases. In the first one, the two waves assumed propagate at the same speed. Under appropriate geometric conditions, we had proved that the energy decays exponentially. While in the second case, when the waves propagate at different speeds, under appropriate geometric conditions, we had proved that the energy decays only at a polynomial rate. In this paper, we confirmed these two results in a 1D numerical approximation. However, when the coupling region does not intersect the damping region, the stabilization of the system is still theoretically an open problem. But, here in both cases, we observed an unpredicted behavior : the energy decays at an exponential rate when the propagation speeds are the same or at a polynomial rate when they are different.

CONTENTS

| | | |
|----------|---|-----------|
| 1 | Introduction | 1 |
| 2 | Finite difference scheme in one dimensional space | 2 |
| 2.1 | Construction of the numerical scheme | 3 |
| 2.2 | Practical implementation and CFL condition | 3 |
| 2.3 | Discrete energy: definition and dissipation | 5 |
| 3 | Numerical experiments: validation of the theoretical results | 6 |
| 3.1 | Same propagation speed: $\mathbf{a} = \mathbf{1}$ | 6 |
| 3.1.1 | No damping: conservation of the total energy | 7 |
| 3.1.2 | $\omega_b \cap \omega_{c_+} \neq \emptyset$. Exponential stability | 7 |
| 3.1.3 | $\omega_b \cap \omega_{c_+} = \emptyset$. Unpredicted behavior | 7 |
| 3.2 | Different propagation speed: $\mathbf{a} > \mathbf{1}$ | 7 |
| 3.2.1 | $\omega_b \cap \omega_{c_+} \neq \emptyset$. Polynomial stability | 7 |
| 3.2.2 | $\omega_b \cap \omega_{c_+} = \emptyset$. Unpredicted behavior | 8 |
| 3.3 | Different propagation speed: $\mathbf{a} < \mathbf{1}$ | 8 |
| 3.3.1 | $\omega_b \cap \omega_{c_+} \neq \emptyset$. Polynomial stability | 8 |
| 3.3.2 | $\omega_b \cap \omega_{c_+} = \emptyset$: Unpredicted behavior | 9 |
| | Acknowledgments | 9 |
| | References | 18 |

1. INTRODUCTION

In [3, 4], the authors considered the stabilization of locally coupled wave equations. The system is described by

$$(1.1) \quad \begin{cases} u_{tt} - a\Delta u + c(x)u_t + b(x)y_t & = 0 & \text{in } \Omega \times \mathbb{R}_+^* \\ y_{tt} - \Delta y - b(x)u_t & = 0 & \text{in } \Omega \times \mathbb{R}_+^* \\ u = y & = 0 & \text{on } \Gamma \times \mathbb{R}_+^*. \end{cases}$$

2010 *Mathematics Subject Classification.* 35L10, 35B40, 93D15, 90D20.

Key words and phrases. Coupled wave equations, internal damping, exact controllability.

where Ω is a nonempty connected open subset of \mathbb{R}^N having a boundary Γ of class C^2 , $a > 0$ constant, $b \in C^0(\Omega, \mathbb{R})$ and $c \in C^0(\Omega, \mathbb{R}^+)$. In [4], the authors established an exponential energy decay rate of System (1.1) provided that the coupling and the damping regions have non empty intersection satisfying the Piecewise Multiplier Geometric Condition (introduced in [5], and recalled in Definition 2 in [3] and denoted by PMGC in short) and that the waves propagate at the same speed (i.e. $a = 1$). This result generalize, in the linear case, that of [1] in the sense that the coupling coefficient function b is not necessarily assumed to be positive and small enough. This result has been generalized in [3] to the case when the coupling region is a subset of the damping region and satisfies a weaker geometric condition namely Geometric Control Condition (introduced in [6], recalled in Definition 1 in [3] and, denoted by GCC in short). Moreover, the stabilization of System (1.1) when the waves are not necessarily propagate at same speed (i.e. $a \neq 1$) has been left as an open problem in [1]. However, in this case (i.e. $a \neq 1$), the lack of exponential stability was proved and the optimal polynomial energy decay rate of type $\frac{1}{t}$ was established under different type of geometric conditions in [3, 4]. Finally, a particular and important case when the coupling region does not intersect the damping region, the stabilization of System (1.1) is still theoretically an open problem.

The purpose of the present work is to focus to confirm numerically these two facts in the 1D model, where geometric conditions are automatically fulfilled, and to numerically study the case when the coupling region and the damping region does not intersect. For this sake, we firstly construct a finite difference numerical approximation of (1.1) in a 1D model. We will construct a suitable discrete energy having the same properties of the continuous energy :

$$E(t) = \frac{1}{2} \int_{\Omega} (|u_t|^2 + a|\nabla u|^2 + |y_t|^2 + |\nabla y|^2) dx.$$

This will allows us to conclude by the numerical study the stabilization of system (1.1).

2. FINITE DIFFERENCE SCHEME IN ONE DIMENSIONAL SPACE

This section is devoted to the numerical approximation of the problem that we considered by a finite difference discretization and to the validation of the theoretical results stated in [3, 4]. We will firstly construct in detail a discretization in the 1D case and we will define its corresponding discrete energy. Numerical experiments are performed to validate the theoretical results. In fact, the numerical results in 1D show an exponential stabilization in any case when $a = 1$ and a polynomial stabilization in any case in the case $a \neq 1$. They are better than expected.

We firstly introduce the finite difference scheme we will work on. Then we will construct the corresponding energy and finally we will perform numerical experiments. Let us firstly recall the problem we are considered.

Consider $\Omega = [0, 1]$. We are interested to study the stabilization of the following coupled wave equations by velocities:

$$(2.1) \quad \begin{cases} u_{tt} - au_{xx} + b(x)y_t + c(x)u_t & = 0 & x \in (0, 1), t > 0 \\ y_{tt} - y_{xx} - b(x)u_t & = 0 & x \in (0, 1), t > 0 \\ u(0, t) = u(1, t) = y(0, t) = y(1, t) & = 0 & t > 0, \end{cases}$$

with the following initial data

$$(2.2) \quad u(x, 0) = u_0(x), \text{ and } y(x, 0) = y_0(x) \quad x \in (0, 1)$$

and

$$(2.3) \quad u_t(x, 0) = u_1(x) \text{ and } y_t(x, 0) = y_1(x), \quad x \in (0, 1)$$

where $a > 0$ constant, $b \in C^0([0, 1], \mathbb{R})$ and $c \in C^0([0, 1], \mathbb{R}^+)$. We will study the two cases $a = 1$ and $a \neq 1$.

2.1. Construction of the numerical scheme. Let N be a non negative integer. Consider the subdivision of $[0, 1]$ given by

$$0 = x_0 < x_1 < \dots < x_N < x_{N+1} = 1, \quad \text{i.e. } x_j = j\Delta x, \quad j = 0, \dots, N+1.$$

Set $t^{n+1} - t^n = \Delta t$ for all $n \in \mathbb{N}$. For $j = 0, \dots, N+1$, we denote $b_j = b(x_j)$, $c_j = c(x_j)$. The explicit finite-difference discretization of system (2.1) is thus, for $n \in \mathbb{N}$ and $j = 1, \dots, N$:

$$(2.4) \quad \begin{cases} \frac{u_j^{n+1} - 2u_j^n + u_j^{n-1}}{\Delta t^2} - a \frac{u_{j+1}^n - 2u_j^n + u_{j-1}^n}{\Delta x^2} + b_j \frac{y_j^{n+1} - y_j^{n-1}}{2\Delta t} + c_j \frac{u_j^{n+1} - u_j^{n-1}}{2\Delta t} = 0 \\ \frac{y_j^{n+1} - 2y_j^n + y_j^{n-1}}{\Delta t^2} - \frac{y_{j+1}^n - 2y_j^n + y_{j-1}^n}{\Delta x^2} - b_j \frac{u_j^{n+1} - u_j^{n-1}}{2\Delta t} = 0. \\ u_0^n = u_{N+1}^n = 0 \\ y_0^n = y_{N+1}^n = 0 \end{cases}$$

According to the initial conditions given by equations (2.2), we have firstly: for $j = 1, \dots, N$,

$$(2.5) \quad u_j^0 = u_0(x_j)$$

$$(2.6) \quad y_j^0 = y_0(x_j).$$

We can use the second initial conditions (2.3) to find the values of u and y at time $t^1 = \Delta t$, by employing a ‘‘ghost’’ time-boundary (i.e. $t^{-1} = -\Delta t$) and the second-order central difference formula for $j = 1, \dots, N$:

$$(2.7) \quad u_1(x_j) = \frac{\partial u}{\partial t} \Big|_{x_j, 0} = \frac{u_j^1 - u_j^{-1}}{2\Delta t} + O(\Delta t^2).$$

Thus we have for $j = 1, \dots, N$:

$$(2.8) \quad u_j^{-1} = u_j^1 - 2\Delta t u_1(x_j).$$

We use the same discrete form of the initial conditions for y , for $j = 1, \dots, N$:

$$(2.9) \quad y_j^{-1} = y_j^1 - 2\Delta t y_1(x_j).$$

Setting $n = 0$, in the numerical scheme (2.4), the two preceding equalities permit us to compute $(u_j^1, y_j^1)_{j=0, N}$. Finally, the solution (u, y) can be computed at any time t^n .

2.2. Practical implementation and CFL condition. Let us denote $\lambda = \frac{\Delta t^2}{\Delta x^2}$. We easily remark that the discrete scheme (2.4) is composed of N linear systems of two equations which can be written under the form:

$$(2.10) \quad \text{for } j = 1, \dots, N, \quad M_j \cdot \begin{pmatrix} u_j^{n+1} \\ y_j^{n+1} \end{pmatrix} = \begin{pmatrix} A_j \\ B_j \end{pmatrix}$$

where

$$M_j = \begin{pmatrix} 1 + \frac{c_j \Delta t}{2} & \frac{b_j \Delta t}{2} \\ -\frac{b_j \Delta t}{2} & 1 \end{pmatrix}$$

$$A_j = 2(1 - a\lambda)u_j^n + \left(\frac{c_j}{2}\Delta t - 1\right)u_j^{n-1} + a\lambda(u_{j+1}^n + u_{j-1}^n) + \frac{b_j}{2}\Delta t y_j^{n-1}$$

and

$$B_j = 2(1 - \lambda)y_j^n + \lambda(y_{j+1}^n + y_{j-1}^n) - y_j^{n-1} - \frac{b_j}{2}\Delta t u_j^{n-1}.$$

Thanks to the hypothesis $\forall x \in (0, 1)$, $c(x) \geq 0$, for $j = 1, \dots, N$ the determinant of M_j given by

$$|M_j| = 1 + \frac{c_j \Delta t}{2} + \left(\frac{b_j \Delta t}{2} \right)^2,$$

is a strictly positive quantity.

Consequently, system (2.10) admits a unique solution given by: for $j = 1, \dots, N$,

$$(2.11) \quad \begin{aligned} u_j^{n+1} &= (1 - a\lambda)\alpha_j u_j^n + \lambda\beta_j(u_{j+1}^n + u_{j-1}^n) + \gamma_j u_j^{n-1} - (1 - \lambda)\varrho_j y_j^n \\ &\quad - \lambda\xi_j(y_{j+1}^n + y_{j-1}^n) + \kappa_j y_j^{n-1} \end{aligned}$$

$$(2.12) \quad \begin{aligned} y_j^{n+1} &= (1 - \lambda)\tilde{\alpha}_j y_j^n + \lambda\tilde{\beta}_j(y_{j+1}^n + y_{j-1}^n) + \tilde{\gamma}_j y_j^{n-1} + (1 - a\lambda)\tilde{\varrho}_j u_j^n \\ &\quad + \lambda\tilde{\xi}_j(u_{j+1}^n + u_{j-1}^n) + \tilde{\kappa}_j u_j^{n-1} \end{aligned}$$

where we have set:

$$\begin{aligned} \alpha_j &= \frac{2}{1 + \frac{c_j}{2}\Delta t + \left(\frac{b_j \Delta t}{2}\right)^2}, & \beta_j &= \frac{a}{1 + \frac{c_j}{2}\Delta t + \left(\frac{b_j \Delta t}{2}\right)^2}, \\ \gamma_j &= \frac{\frac{c_j}{2}\Delta t + \left(\frac{b_j \Delta t}{2}\right)^2 - 1}{1 + \frac{c_j}{2}\Delta t + \left(\frac{b_j \Delta t}{2}\right)^2}, & \varrho_j &= \frac{b_j \Delta t}{1 + \frac{c_j}{2}\Delta t + \left(\frac{b_j \Delta t}{2}\right)^2}, \\ \xi_j &= \frac{b_j \Delta t}{2 \left(1 + \frac{c_j}{2}\Delta t + \left(\frac{b_j \Delta t}{2}\right)^2\right)}, & \kappa_j &= \frac{b_j \Delta t}{1 + \frac{c_j}{2}\Delta t + \left(\frac{b_j \Delta t}{2}\right)^2}, \\ \tilde{\alpha}_j &= 2 - \frac{(b_j \Delta t)^2}{2 \left(1 + \frac{c_j}{2}\Delta t + \left(\frac{b_j \Delta t}{2}\right)^2\right)}, & \tilde{\beta}_j &= 1 - \frac{(b_j \Delta t)^2}{4 \left(1 + \frac{c_j}{2}\Delta t + \left(\frac{b_j \Delta t}{2}\right)^2\right)}, \\ \tilde{\gamma}_j &= \frac{(b_j \Delta t)^2}{2 \left(1 + \frac{c_j}{2}\Delta t + \left(\frac{b_j \Delta t}{2}\right)^2\right)} - 1, & \tilde{\varrho}_j &= \frac{b_j \Delta t}{1 + \frac{c_j}{2}\Delta t + \left(\frac{b_j \Delta t}{2}\right)^2}, \\ \tilde{\xi}_j &= \frac{ab_j \Delta t}{2 \left(1 + \frac{c_j}{2}\Delta t + \left(\frac{b_j \Delta t}{2}\right)^2\right)}, & \tilde{\kappa}_j &= \left[\frac{\frac{c_j}{2}\Delta t + \left(\frac{b_j \Delta t}{2}\right)^2 - 1}{1 + \frac{c_j}{2}\Delta t + \left(\frac{b_j \Delta t}{2}\right)^2} - 1 \right] \frac{b_j \Delta t}{2}. \end{aligned}$$

The implementation of the numerical discretization of the problem (2.1) consists finally of equations (2.5), (2.6), (2.11), (2.12) where (u^{-1}, y^{-1}) used for $n = 0$, are defined by (2.8), (2.9).

By a standard von Neumann stability analysis (that is a discrete Fourier analysis, see for instance [2]), the numerical scheme is stable if and only if, the following Courant-Friedrichs-Lewy, CFL, condition holds:

$$\Delta t^2 \leq \Delta x^2 \text{ and } a \Delta t^2 \leq \Delta x^2$$

which is equivalent to

$$(2.13) \quad \Delta t \leq \min \left(1, \frac{1}{\sqrt{a}} \right) \Delta x.$$

The number $\min \left(1, \frac{1}{\sqrt{a}} \right)$ is called the CFL number and is denoted in the following by CFL .

2.3. Discrete energy: definition and dissipation. The aim of this section is to design a discrete energy that might be preserved in the case $c = 0$ and to obtain the dissipation of the discrete energy in the case $c > 0$. To this end, let us define:

- the discrete kinetic energy for u as: $E_{k,u}^n = \frac{1}{2} \sum_{j=1}^N \left(\frac{u_j^{n+1} - u_j^n}{\Delta t} \right)^2$
- the discrete potential energy for u as: $E_{p,u}^n = \frac{a}{2} \sum_{j=0}^N \left(\frac{u_{j+1}^n - u_j^n}{\Delta x} \right) \left(\frac{u_{j+1}^{n+1} - u_j^{n+1}}{\Delta x} \right)$
- the discrete kinetic energy for y as: $E_{k,y}^n = \frac{1}{2} \sum_{j=1}^N \left(\frac{y_j^{n+1} - y_j^n}{\Delta t} \right)^2$
- the discrete potential energy for u as: $E_{y,u}^n = \frac{1}{2} \sum_{j=0}^N \left(\frac{y_{j+1}^n - y_j^n}{\Delta x} \right) \left(\frac{y_{j+1}^{n+1} - y_j^{n+1}}{\Delta x} \right)$

The total discrete energy is then defined as

$$(2.14) \quad \mathcal{E}^n = E_{k,u}^n + E_{p,u}^n + E_{k,y}^n + E_{y,u}^n.$$

Let us prove now that this definition of the energy fulfills the two properties stated above. For this sake, we multiply the first equation of (2.4) by $(u_j^{n+1} - u_j^{n-1})$ and we sum over $j = 1, \dots, N$. We obtain:

$$(2.15) \quad \begin{aligned} & \sum_{j=1}^N \frac{u_j^{n+1} - 2u_j^n + u_j^{n-1}}{\Delta t^2} (u_j^{n+1} - u_j^{n-1}) - a \sum_{j=1}^N \frac{u_{j+1}^n - 2u_j^n + u_{j-1}^n}{\Delta x^2} (u_j^{n+1} - u_j^{n-1}) \\ & + \sum_{j=1}^N b_j \frac{y_j^{n+1} - y_j^{n-1}}{2\Delta t} (u_j^{n+1} - u_j^{n-1}) + \sum_{j=1}^N c_j \frac{(u_j^{n+1} - u_j^{n-1})^2}{2\Delta t} = 0. \end{aligned}$$

Estimation of the first term of (2.15) We firstly have:

$$(2.16) \quad \begin{aligned} \sum_{j=1}^N \frac{u_j^{n+1} - 2u_j^n + u_j^{n-1}}{\Delta t^2} (u_j^{n+1} - u_j^{n-1}) &= \sum_{j=1}^N \frac{u_j^{n+1} - u_j^n - (u_j^n - u_j^{n-1})}{\Delta t^2} (u_j^{n+1} - u_j^n + u_j^n - u_j^{n-1}) \\ &= \sum_{j=1}^N \left(\frac{u_j^{n+1} - u_j^n}{\Delta t} \right)^2 - \sum_{j=1}^N \left(\frac{u_j^{n+1} - u_j^{n-1}}{\Delta t} \right)^2 \\ &= 2(E_{k,u}^n - E_{k,u}^{n-1}). \end{aligned}$$

Estimation of the second term of (2.15). Using the same trick we have:

$$\begin{aligned} -a \sum_{j=1}^N \frac{u_{j+1}^n - 2u_j^n + u_{j-1}^n}{\Delta x^2} (u_j^{n+1} - u_j^{n-1}) &= -a \sum_{j=1}^N \frac{u_{j+1}^n - u_j^n - (u_j^n - u_{j-1}^n)}{\Delta x^2} (u_j^{n+1} - u_j^{n-1}) \\ &= -a \sum_{j=1}^N \frac{(u_{j+1}^n - u_j^n)(u_j^{n+1} - u_j^{n-1})}{\Delta x^2} \\ &\quad + a \sum_{j=1}^{N+1} \frac{(u_j^n - u_{j-1}^n)(u_j^{n+1} - u_j^{n-1})}{\Delta x^2}. \end{aligned}$$

So, by translation of index in the second term in the previous sum, we will have:

$$\begin{aligned} -a \sum_{j=1}^N \frac{u_{j+1}^n - 2u_j^n + u_{j-1}^n}{\Delta x^2} (u_j^{n+1} - u_j^{n-1}) &= -a \sum_{j=0}^N \frac{(u_{j+1}^n - u_j^n)(u_j^{n+1} - u_j^{n-1})}{\Delta x^2} \\ &\quad + a \sum_{j=0}^N \frac{(u_{j+1}^n - u_j^n)(u_{j+1}^{n+1} - u_{j+1}^{n-1})}{\Delta x^2} \end{aligned}$$

$$\begin{aligned}
-a \sum_{j=1}^N \frac{u_{j+1}^n - 2u_j^n + u_{j-1}^n}{\Delta x^2} (u_j^{n+1} - u_j^{n-1}) &= a \sum_{j=0}^N \frac{(u_{j+1}^{n+1} - u_j^{n+1})(u_{j+1}^n - u_j^n)}{\Delta x^2} \\
&- a \sum_{j=0}^N \frac{(u_{j+1}^{n-1} - u_j^{n-1})(u_{j+1}^n - u_j^n)}{\Delta x^2} \\
(2.17) \qquad \qquad \qquad &= 2(E_{p,u}^n - E_{p,u}^{n-1}).
\end{aligned}$$

Substituting (2.16) and (2.17) into (2.15), we get

$$\begin{aligned}
2 \left(E_{k,u}^n + E_{p,u}^n - E_{k,u}^{n-1} - E_{p,u}^{n-1} \right) + 2\Delta t \sum_{j=1}^N c_j \left(\frac{u_j^{n+1} - u_j^{n-1}}{2\Delta t} \right)^2 \\
(2.18) \qquad \qquad \qquad + \sum_{j=1}^N b_j \frac{y_j^{n+1} - y_j^{n-1}}{2\Delta t} (u_j^{n+1} - u_j^{n-1}) = 0.
\end{aligned}$$

Similarly, by multiplying the second equation of (2.4) by $(y_j^{n+1} - y_j^{n-1})$, and using the same algebraic tricks, we will get:

$$(2.19) \qquad 2 \left(E_{k,y}^n + E_{p,y}^n - E_{k,y}^{n-1} - E_{p,y}^{n-1} \right) - \sum_{j=1}^N b_j \frac{u_j^{n+1} - u_j^{n-1}}{2\Delta t} (y_j^{n+1} - y_j^{n-1}) = 0.$$

Using the definition of the total discrete energy, (2.14), and the two equations (2.18), (2.19) leads to:

$$(2.20) \qquad (\mathcal{E}^n - \mathcal{E}^{n-1}) + \Delta t \sum_{j=1}^N c_j \left(\frac{u_j^{n+1} - u_j^{n-1}}{2\Delta t} \right)^2 = 0.$$

Consequently, the total discrete energy of system (2.4) is decreasing along time.

3. NUMERICAL EXPERIMENTS: VALIDATION OF THE THEORETICAL RESULTS

In every experiment, we have chosen:

$$u_0(x) = x(x-1), \quad u_1(x) = x(x-1), \quad y_0(x) = -x(x-1), \quad y_1(x) = -x(x-1).$$

The mesh size is chosen as $N = 100$ so that $\Delta x = 0.01$ and the time step is chosen as $\frac{\Delta t}{\Delta x} = CFL$.

In order to validate the different theoretical results, we have chosen different functions b and c synthesized in the list below:

- No coupling: $b_1(x) = 0$ or no dissipation $c_1(x) = 0$,
- Full coupling $b_2(x) = \mathbb{1}_{(0,1)}(x)$ or full dissipation $c_2(x) = \mathbb{1}_{(0,1)}(x)$,
- Partial coupling $b_3(x) = \mathbb{1}_{[0.1,0.2] \cup [0.8,0.9]}(x)$ or partial dissipation $c_3(x) = \mathbb{1}_{[0.1,0.2] \cup [0.8,0.9]}(x)$,
- Partial coupling $b_4(x) = \mathbb{1}_{[0.1,0.2]}(x)$ or partial dissipation $c_4(x) = \mathbb{1}_{[0.1,0.2]}(x)$,
- Partial coupling $b_5(x) = \mathbb{1}_{[0.4,0.6]}(x)$ or partial dissipation $c_5(x) = \mathbb{1}_{[0.4,0.6]}(x)$.

Combining the different choices of the coupling and damping functions in order to have or not $\omega_b \cap \omega_{c_+} \neq \emptyset$ will permit us to validate the theoretical results.

Let us notice that in the special case of the dimension 1, the geometric control condition GCC holds as soon as $\omega_{c_+} \neq \emptyset$.

3.1. Same propagation speed: $\alpha = 1$. For every numerical simulation, the final time T is chosen as $T = 500$.

3.1.1. *No damping: conservation of the total energy.* Firstly, let us verify that when no damping are present, the discrete energy is conserved. We present in figure 2 the numerical experiment when $c = c_1 = 0$ and $b = b_3 = \mathbb{1}_{[0.1,0.2] \cup [0.8,0.9]}(x)$. Indeed, the total energy is conserved along time.

Remark 1. This numerical test where no damping is applied shows that without a damping term, the total energy is completely conserved. This fact suggests that the numerical scheme does not produce numerical dissipation. So the numerical behavior observed thereafter is only due to the considered model.

3.1.2. $\omega_b \cap \omega_{c_+} \neq \emptyset$. *Exponential stability.* Let us now verify the theoretical results when we suppose that $\omega_b \cap \omega_{c_+} \neq \emptyset$. For this sake, we present in figure 3, the total energy and the quantity $-\ln(E(t))/t$ versus time t for large time, where we have chosen $b = b_4(x) = \mathbb{1}_{[0.1,0.2]}(x)$ and $c = c_3(x) = \mathbb{1}_{[0.1,0.2] \cup [0.8,0.9]}(x)$. This choice verifies the assumption that $\omega_b \cap \omega_{c_+} \neq \emptyset$ and in figure 3, it is shown that the energy is decreasing and an exponential decay is observed since it seems that $-\ln(E(t))/t$ tends to a constant as $t \rightarrow +\infty$. The final time profile confirms that u and y are small and the final profiles of u and y are smooth as expected (high frequency oscillations are exponentially dissipated).

3.1.3. $\omega_b \cap \omega_{c_+} = \emptyset$. *Unpredicted behavior.* At the numerical level, we are interested in the long time behavior of the solution (u, y) when we suppose that $\omega_b \cap \omega_{c_+} = \emptyset$. For this sake, we present in figure 4, the total energy and the quantity $-\ln(E(t))/t$ versus time t for large time, where we have chosen $b = b_4(x) = \mathbb{1}_{[0.1,0.2]}(x)$ and $c = c_5(x) = \mathbb{1}_{[0.4,0.6]}(x)$. This choice verifies the assumption that $\omega_b \cap \omega_{c_+} = \emptyset$. In figure 4, it is shown that the energy is decreasing and an exponential decay is observed since it seems that $-\ln(E(t))/t$ tends to a constant as $t \rightarrow +\infty$. The final time profile confirms that u and y are small and again the couple of solution (u, y) is smooth. We have not considered this case in the theoretical study and this numerical result shows a similar behavior as in the case presented before.

So we decided to confirm this behavior by choosing $b = b_5(x) = \mathbb{1}_{[0.4,0.6]}(x)$ and $c = c_4(x) = \mathbb{1}_{[0.1,0.2]}(x)$. This choice verifies also the assumption that $\omega_b \cap \omega_{c_+} = \emptyset$. In figure 5, it is shown that the energy is decreasing and an exponential decay is observed since it seems that $-\ln(E(t))/t$ tends to a constant as $t \rightarrow +\infty$. The final time profile confirms that u and y are small and again the couple of solution (u, y) is smooth.

Remark 2. Let us notice that when the propagation speeds are the same for u and y , the final profiles of the solution u, y presented in figure 3c, figure 4c and in figure 5c have the same form as the initial one, that is no spurious oscillations due to high frequency are present.

3.2. **Different propagation speed: $a > 1$.** We investigate now the long time behavior of (u, y) when the propagation speeds are different and specifically when $a > 1$. So we have chosen to take $a = 2$. We firstly investigate the case when the propagation speed for u is greater than the one of y namely $a > 1$. We have chosen $a = 2$.

3.2.1. $\omega_b \cap \omega_{c_+} \neq \emptyset$. *Polynomial stability.* Let us now verify the theoretical results when we suppose that $\omega_b \cap \omega_{c_+} \neq \emptyset$. For this sake, we present in figure 6, the total energy where we have chosen $b = b_4(x) = \mathbb{1}_{[0.1,0.2]}(x)$ and $c = c_3(x) = \mathbb{1}_{[0.1,0.2] \cup [0.8,0.9]}(x)$.

When taking as final time $T = 500$, it seems that the energy does not tend to zero as shown in figure 6a. This is the reason why we have chosen for the case when $a \neq 1$ as final time $T = 500\,000$ and figure 6b shows that the energy finally goes to zero.

To explore the speed of convergence to zero, we have plotted in figure 7 $-\ln(E(t))/t$, $t \cdot E(t)$ and finally $-\ln(E(t))/\ln(t)$ versus t . Figure 7a shows clearly that $-\ln(E(t))/t$ tends to zero and it permits to conclude that $E(t)$ tends to zero slower than an exponential. Figure 7b permits to conclude that $E(t)$ tends to zero faster than $1/t$. Finally figure 7c shows that $E(t)$ tends to zero as $1/t^\alpha$ with $\alpha \simeq 1.4$.

The final time profile presented in figure 7d confirms that u and y are small but it shows also that high frequencies for the unknown y are not completely controlled.

3.2.2. $\omega_b \cap \omega_{c_+} = \emptyset$. Unpredicted behavior. At the numerical level, we are interested in the long time behavior of the solution (u, y) when we suppose that $\omega_b \cap \omega_{c_+} = \emptyset$. For this sake, we present in figure 8, the total energy where we have chosen $b = b_4(x) = \mathbb{1}_{[0.1,0.2]}(x)$ and $c = c_5(x) = \mathbb{1}_{[0.4,0.6]}(x)$.

Again, when taking as final time $T = 500$, it seems that the energy does not tend to zero as shown in figure 8a. Taking as final time $T = 500\,000$, figure 8b shows that the energy goes finally to zero.

To explore the speed of convergence to zero, we have plotted in figure 9 $-\ln(E(t))/t$, $t \cdot E(t)$ and finally $-\ln(E(t))/\ln(t)$ versus t . Figure 9a shows clearly that $-\ln(E(t))/t$ tends to zero and it permits to conclude that $E(t)$ tends to zero slower than an exponential but figure 9b shows that $E(t)$ tends to zero slower than $1/t$. This fact is confirmed by figure 9c which shows that $E(t)$ tends to zero as $1/t^\alpha$ with $\alpha \simeq 0.9$. Eventually, taking a larger time could conclude that the convergence is like $1/t$.

Again, the final time profile presented in figure 9d confirms that u and y are small but it shows also that high frequencies for the unknown y are not completely controlled.

As for the case when the two propagation speeds were identical this results was not predicted by the theoretical results.

So we decided to confirm this behavior by choosing $b = b_5(x) = \mathbb{1}_{[0.4,0.6]}(x)$ and $c = c_4(x) = \mathbb{1}_{[0.1,0.2]}(x)$. Again, when taking as final time $T = 500$, it seems that the energy does not tends to zero as shown in figure 10a. Taking as final time $T = 500\,000$, figure 8b shows that the energy goes finally to zero.

To explore the speed of convergence to zero, we have plotted in figure 11 $-\ln(E(t))/t$, $t \cdot E(t)$ and finally $-\ln(E(t))/\ln(t)$ versus t . Figure 11a shows clearly that $-\ln(E(t))/t$ tends to zero and it permits to conclude that $E(t)$ tends to zero slower than an exponential and figure 11b permits to conclude that the convergence is faster than $1/t$. Finally figure 11c shows that $E(t)$ tends to zero as $1/t^\alpha$ with $\alpha \simeq 1.19$.

Remark 3. The final time profile presented in figure 7d, figure 9d and figure 11d confirms that u and y are small but it shows also that high frequencies for the unknown y are not completely controlled.

3.3. Different propagation speed: $a < 1$. When $a \neq 1$, in order to see if the same behavior occurs no matter if a is greater or less than 1, we investigate now the long time behavior of (u, y) when the propagation speeds is less than the one of y namely $a < 1$. We have chosen $a = 0.5$.

3.3.1. $\omega_b \cap \omega_{c_+} \neq \emptyset$. Polynomial stability. Let us now verify the theoretical results when we suppose that $\omega_b \cap \omega_{c_+} \neq \emptyset$. For this sake, we present in figure 12a, the total energy where we have chosen $b = b_4(x) = \mathbb{1}_{[0.1,0.2]}(x)$ and $c = c_3(x) = \mathbb{1}_{[0.1,0.2] \cup [0.8,0.9]}(x)$.

When taking as final time $T = 500$, it seems that the energy does not tend to zero as shown in figure 12a. Taking as final time $T = 500\,000$, figure 12b shows that the energy goes finally to zero.

To explore the speed of convergence to zero, we have plotted in figure 13 $-\ln(E(t))/t$, $t \cdot E(t)$ and finally $-\ln(E(t))/\ln(t)$ versus t . Figure 13a shows clearly that $-\ln(E(t))/t$ tends to zero slower than an exponential. Figure 13b permits to conclude that $E(t)$ tends to zero faster than $1/t$. Finally figure 13c shows that $E(t)$ tends to zero as $1/t^\alpha$ with $\alpha \simeq 1.5$.

The final time profile confirms that u and y are small but it shows also that high frequencies for the unknown y are not completely controlled.

3.3.2. $\omega_b \cap \omega_{c_+} = \emptyset$: *Unpredicted behavior.* Again, the numerical level, we are interested in the long time behavior of the solution (u, y) when we suppose that $\omega_b \cap \omega_{c_+} = \emptyset$. For this sake, we present in figure 14a, the total energy where we have chosen $b = b_4(x) = \mathbb{1}_{[0.1,0.2]}(x)$ and $c = c_5(x) = \mathbb{1}_{[0.4,0.6]}(x)$.

Again, when taking as final time $T = 500$, it seems that the energy does not tend to zero as shown in figure 14a. Taking as final time $T = 500\,000$, figure 14b shows that the energy finally goes to zero.

To explore the speed of convergence to zero, we have plotted in figure 15 $-\ln(E(t))/t$, $t \cdot E(t)$ and finally $-\ln(E(t))/\ln(t)$ versus t . Figure 15a shows clearly that $-\ln(E(t))/t$ tends to zero slower than an exponential. But figure 15b shows that $E(t)$ tends to zero faster than $1/t$. Finally figure 15c shows that $E(t)$ tends to zero as $1/t^\alpha$ with $\alpha \simeq 1.25$.

Again, the final time profile presented in figure 15d confirms that u and y are small but it shows also that high frequencies for the unknown y are not completely controlled. This result was not predicted by the theoretical results.

So we decided to confirm this behavior by choosing $b = b_5(x) = \mathbb{1}_{[0.4,0.6]}(x)$ and $c = c_4(x) = \mathbb{1}_{[0.1,0.2]}(x)$. Again, when taking as final time $T = 500$, it seems that the energy does not tend to zero as shown in figure 16a. Taking as final time $T = 500\,000$, figure 16b shows that the energy goes finally to zero.

To explore the speed of convergence to zero, we have plotted in figure 17 $-\ln(E(t))/t$, $t \cdot E(t)$ and finally $-\ln(E(t))/\ln(t)$ versus t . Figure 17a shows clearly that $-\ln(E(t))/t$ tends to zero and it permits to conclude that $E(t)$ tends to zero slower than an exponential but figure 17b shows that $E(t)$ tends to zero faster than $1/t$. Finally figure 17c shows that $E(t)$ tends to zero as $1/t^\alpha$ with $\alpha \simeq 1.15$.

Again, the final time profile presented in figure 17d confirms that u and y are small but it shows also that high frequencies for the unknown y are not completely controlled.

Remark 4. The final time profile presented in figure 13d, figure 15d and figure 17d confirms that u and y are small but it shows also that high frequencies for the unknown y are not completely controlled.

Remark 5. When the propagation speeds are not equal, the solution (u, y) has the same behavior no matter if $a > 1$ or $a < 1$. The polynomial convergence is numerically better than $1/t$ but it will be probably be $1/t$ for greater time. For reason of computation time, we did not perform very long simulation to confirm.

Acknowledgments. The authors are grateful to the anonymous referees and the editor for their valuable comments and useful suggestions.

The authors thanks professor Kais Ammari for their valuable discussions and comments.

Amina Mortada and Ch
framework of the PCSI
Problems and Applicatio
Ali Wehbe would like t
Université Savoie Mont

ry for its support in the
y of Some Mathematical
of Mathematics of the

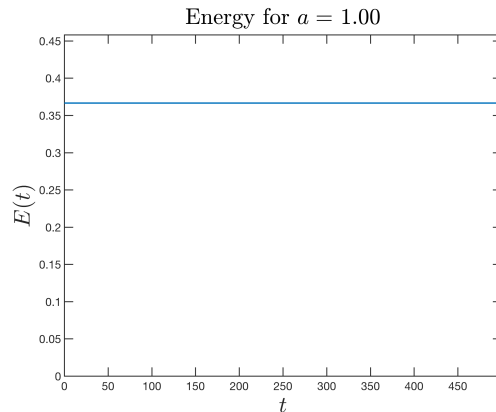


FIGURE 2. No damping.

$$c = c_1 = 0, \text{ partial coupling } b = b_3 = \mathbb{1}_{[0.1,0.2] \cup [0.8,0.9]}(x)$$

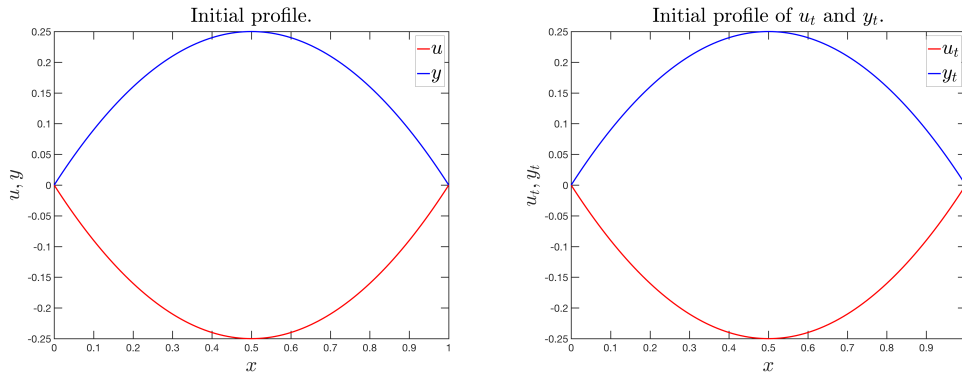
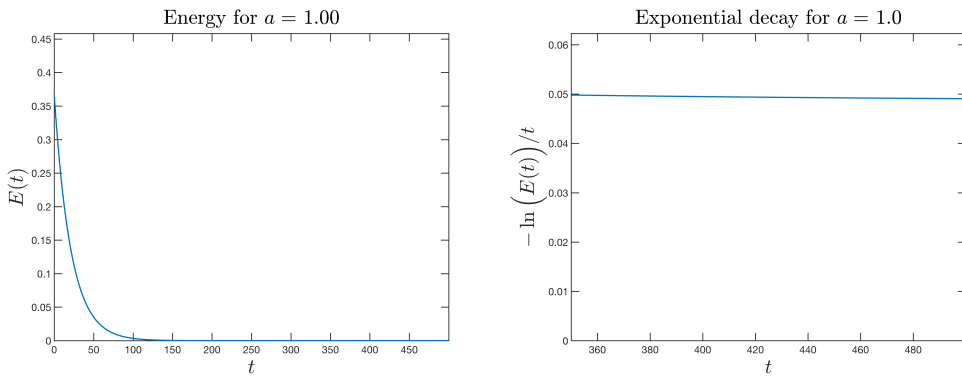
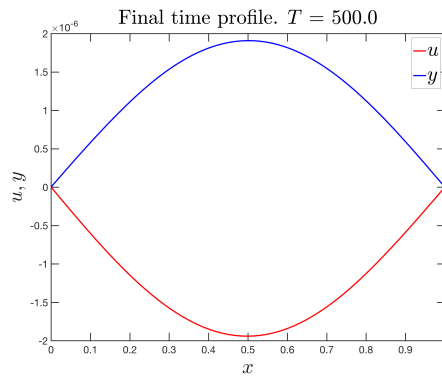


FIGURE 1. Initial profiles



(A) Energy.

(B) Exponential decay.



(C) Final time profile.

FIGURE 3. Long time behavior when $\omega_b \cap \omega_{c_+} \neq \emptyset$.
 $b = b_4(x) = \mathbf{1}_{[0.1, 0.2]}(x)$ and $c = c_3(x) = \mathbf{1}_{[0.1, 0.2] \cup [0.8, 0.9]}(x)$

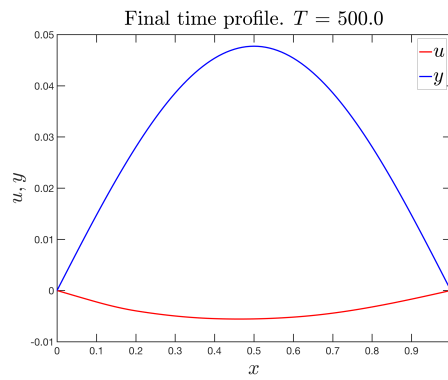
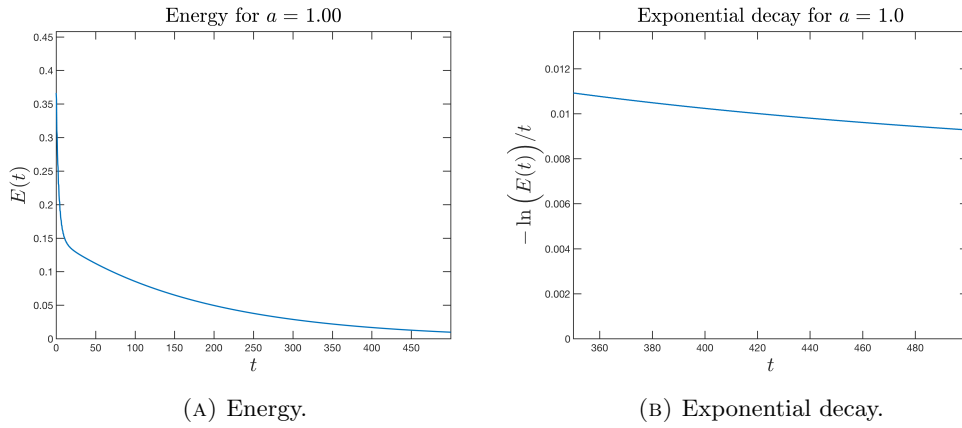
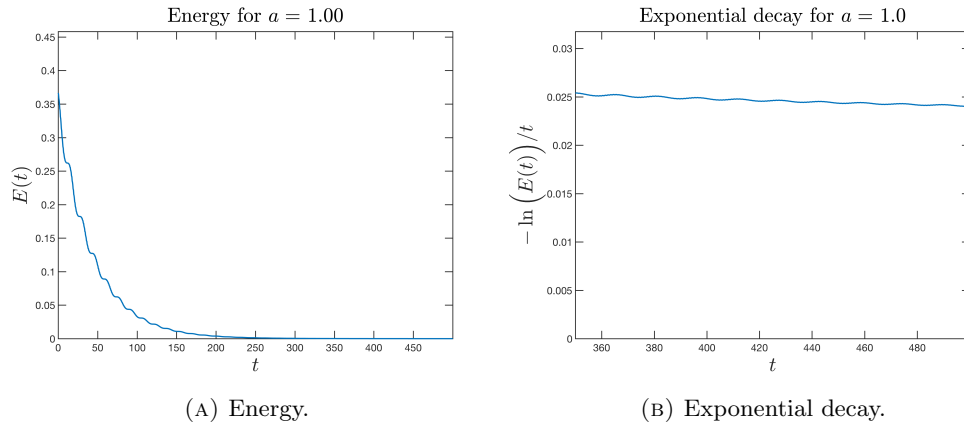
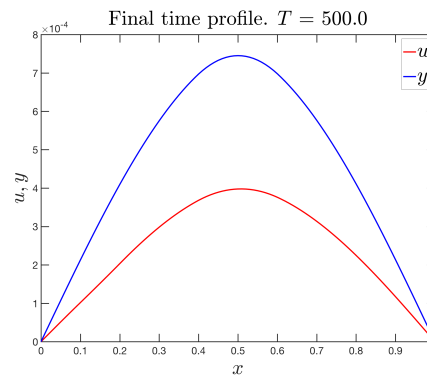


FIGURE 4. Long time behavior when $\omega_b \cap \omega_{c_+} = \emptyset$.
 $b = b_4(x) = \mathbf{1}_{[0.1,0.2]}(x)$ and $c = c_5(x) = \mathbf{1}_{[0.4,0.6]}(x)$



(A) Energy.

(B) Exponential decay.



(C) Final time profile.

FIGURE 5. Long time behavior when $\omega_b \cap \omega_{c_+} = \emptyset$.
 $b = b_5(x) = \mathbf{1}_{[0.4, 0.6]}(x)$ and $c = c_4(x) = \mathbf{1}_{[0.1, 0.2]}(x)$

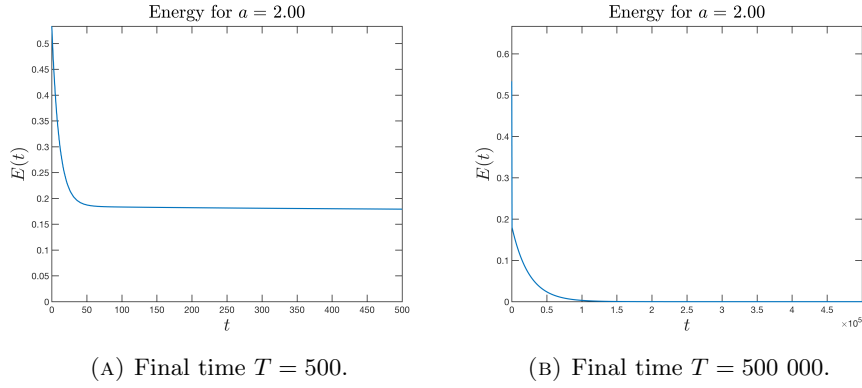


FIGURE 6. Energy when $\omega_b \cap \omega_{c_+} \neq \emptyset$.
 $b = b_4(x) = \mathbb{1}_{[0.1,0.2]}(x)$ and $c = c_3(x) = \mathbb{1}_{[0.1,0.2] \cup [0.8,0.9]}(x)$

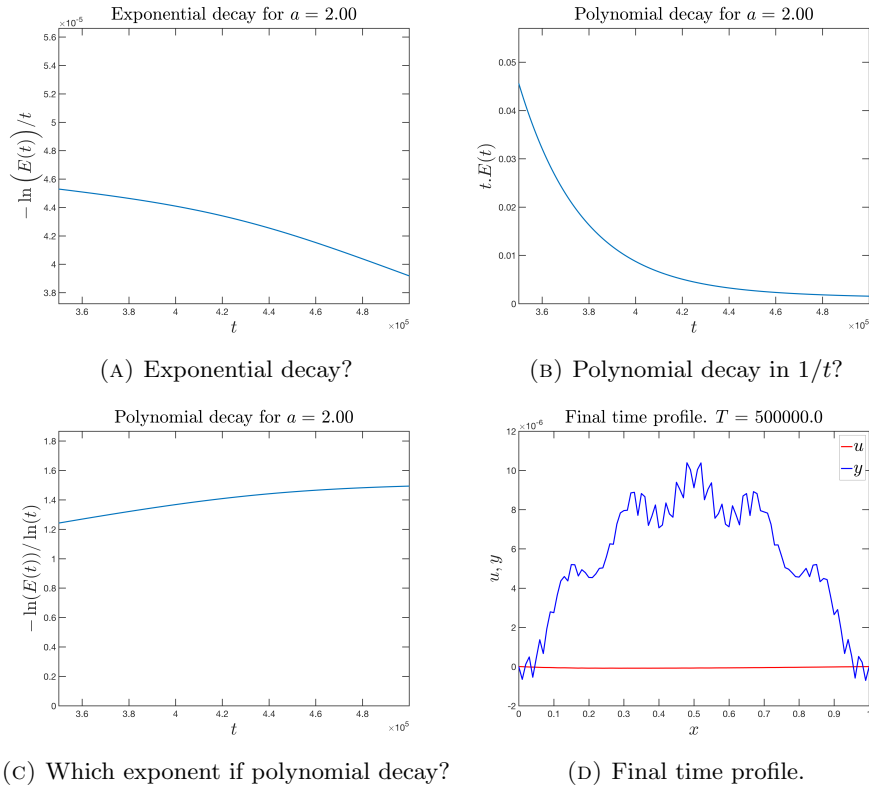


FIGURE 7. Long time behavior when $\omega_b \cap \omega_{c_+} \neq \emptyset$.
 $b = b_4(x) = \mathbb{1}_{[0.1,0.2]}(x)$ and $c = c_3(x) = \mathbb{1}_{[0.1,0.2] \cup [0.8,0.9]}(x)$

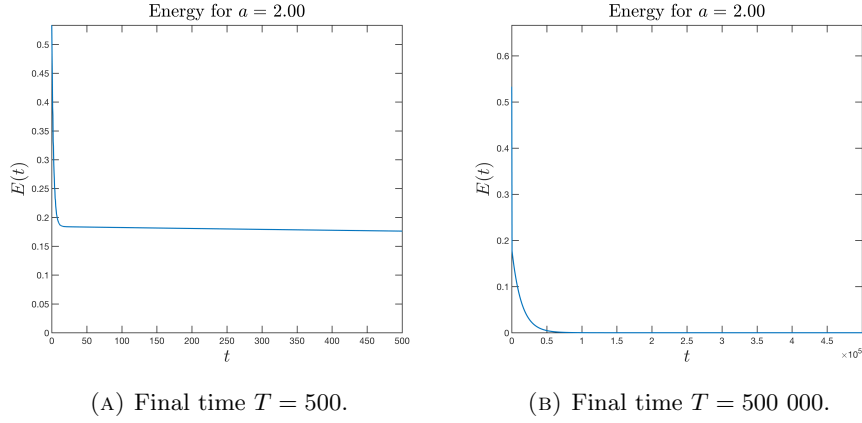


FIGURE 8. Energy when $\omega_b \cap \omega_{c_+} = \emptyset$.
 $b = b_4(x) = \mathbf{1}_{[0.1,0.2]}(x)$ and $c = c_5(x) = \mathbf{1}_{[0.4,0.6]}(x)$

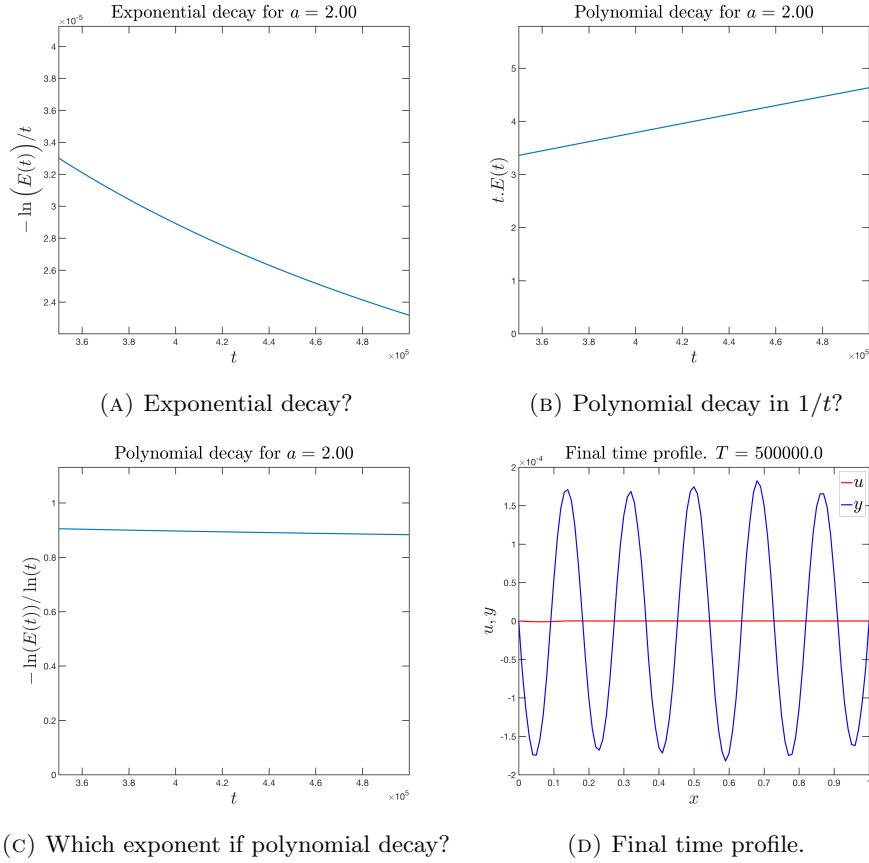


FIGURE 9. Long time behavior when $\omega_b \cap \omega_{c_+} = \emptyset$.
 $b = b_4(x) = \mathbf{1}_{[0.1,0.2]}(x)$ and $c = c_5(x) = \mathbf{1}_{[0.4,0.6]}(x)$

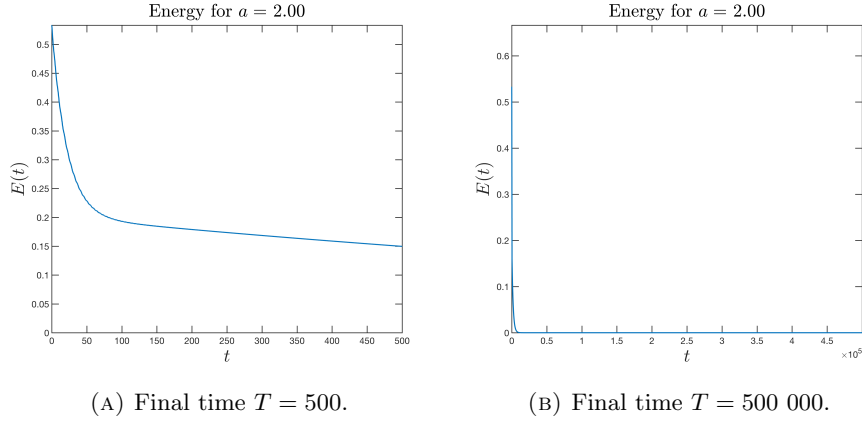


FIGURE 10. Energy when $\omega_b \cap \omega_{c_+} = \emptyset$.
 $b = b_4(x) = \mathbb{1}_{[0.1,0.2]}(x)$ and $c = c_5(x) = \mathbb{1}_{[0.4,0.6]}(x)$

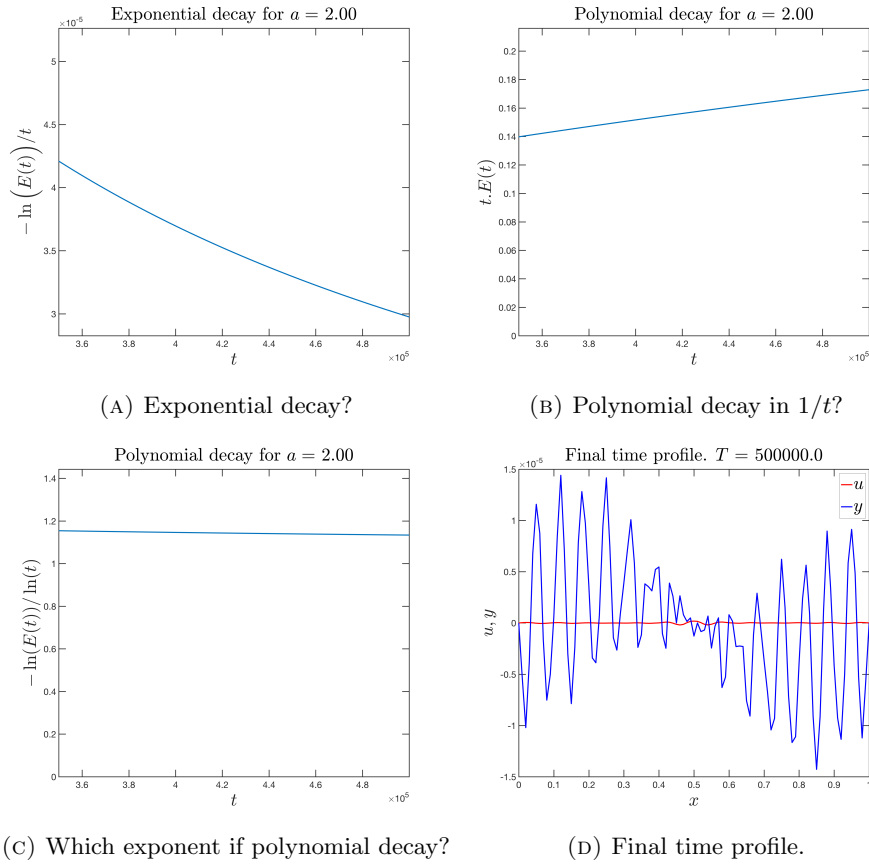


FIGURE 11. Long time behavior when $\omega_b \cap \omega_{c_+} = \emptyset$.
 $b = b_5(x) = \mathbb{1}_{[0.4,0.6]}(x)$ and $c = c_4(x) = \mathbb{1}_{[0.1,0.2]}(x)$

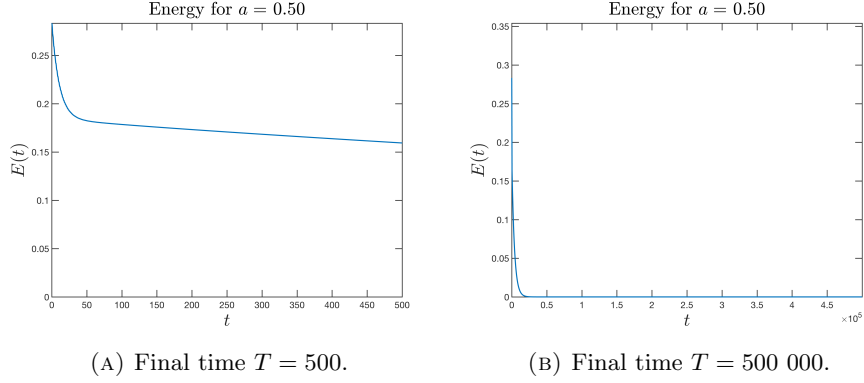


FIGURE 12. Energy when $\omega_b \cap \omega_{c_+} \neq \emptyset$.
 $b = b_4(x) = \mathbb{1}_{[0.1,0.2]}(x)$ and $c = c_3(x) = \mathbb{1}_{[0.1,0.2] \cup [0.8,0.9]}(x)$

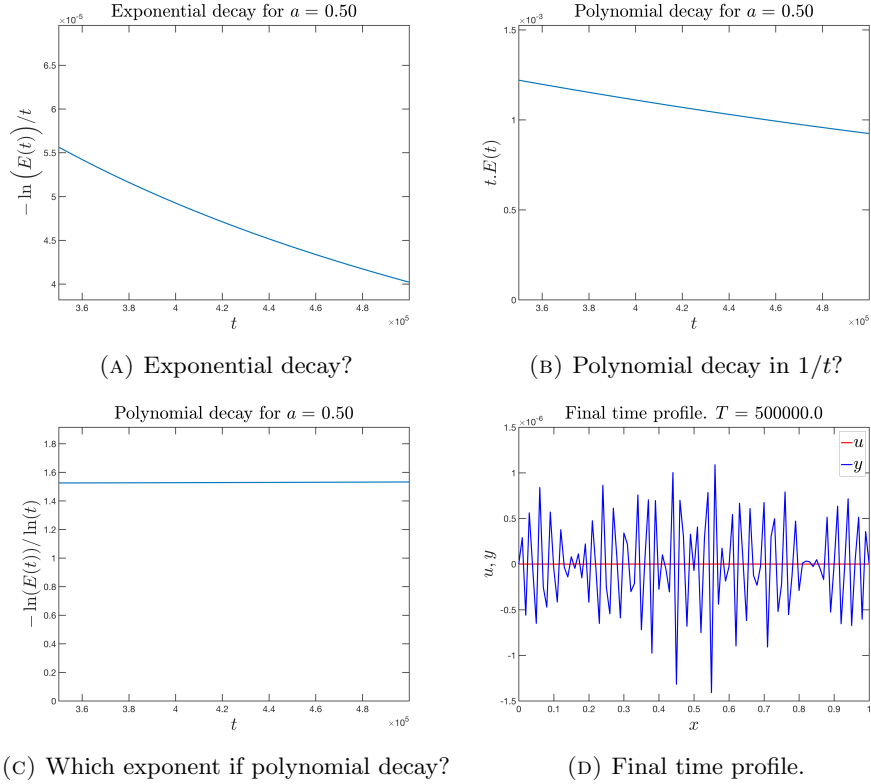


FIGURE 13. Long time behavior when $\omega_b \cap \omega_{c_+} \neq \emptyset$.
 $b = b_4(x) = \mathbb{1}_{[0.1,0.2]}(x)$ and $c = c_3(x) = \mathbb{1}_{[0.1,0.2] \cup [0.8,0.9]}(x)$

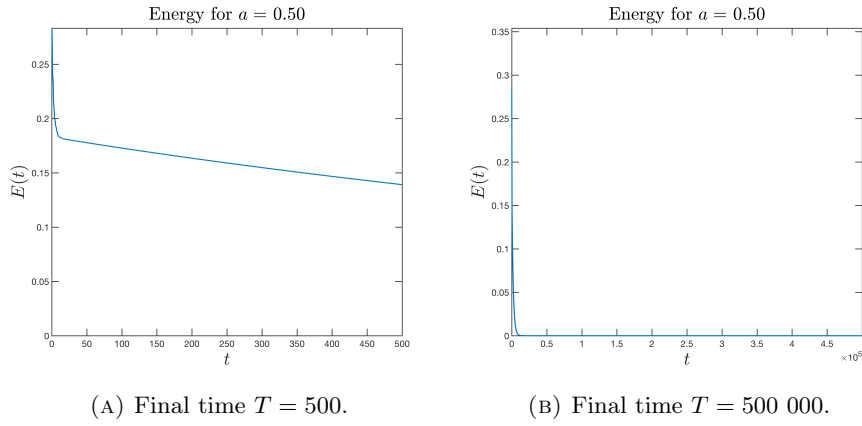


FIGURE 14. Energy when $\omega_b \cap \omega_{c_+} = \emptyset$.
 $b = b_4(x) = \mathbb{1}_{[0.1,0.2]}(x)$ and $c = c_5(x) = \mathbb{1}_{[0.4,0.6]}(x)$

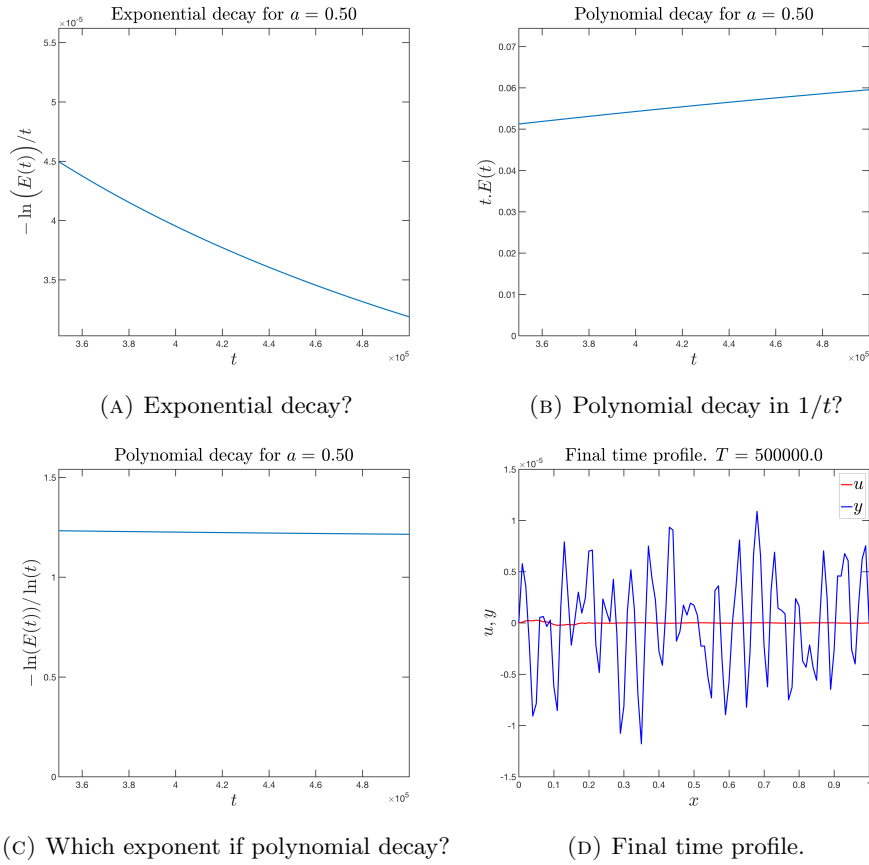


FIGURE 15. Long time behavior when $\omega_b \cap \omega_{c_+} = \emptyset$.
 $b = b_4(x) = \mathbb{1}_{[0.1,0.2]}(x)$ and $c = c_5(x) = \mathbb{1}_{[0.4,0.6]}(x)$

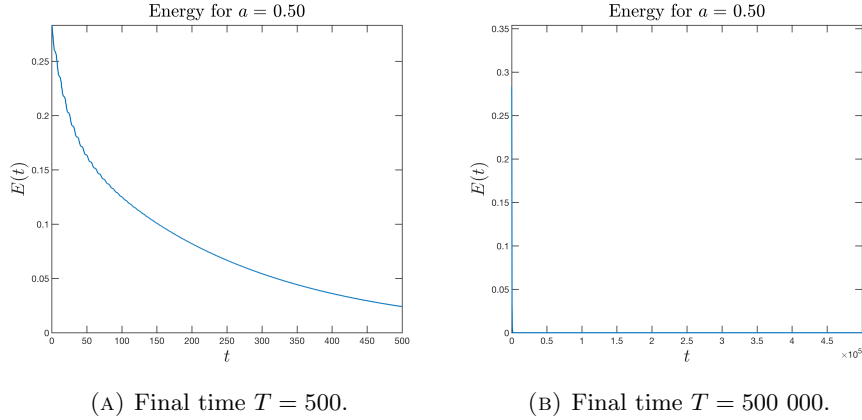


FIGURE 16. Energy when $\omega_b \cap \omega_{c_+} = \emptyset$.
 $b = b_4(x) = \mathbf{1}_{[0.1,0.2]}(x)$ and $c = c_5(x) = \mathbf{1}_{[0.4,0.6]}(x)$

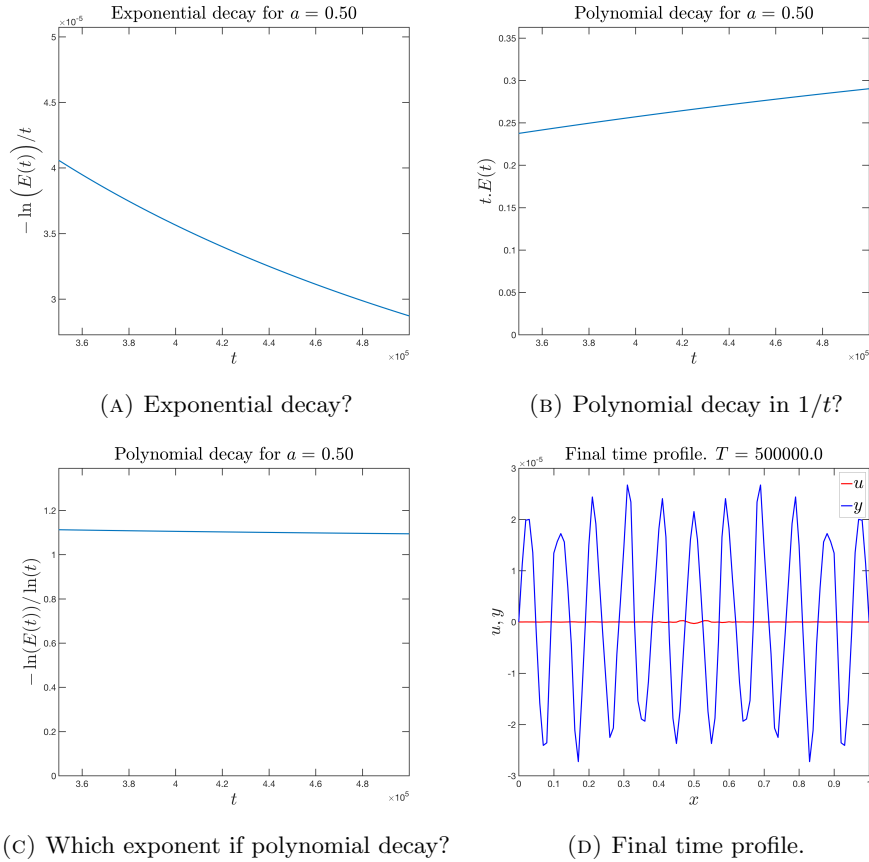


FIGURE 17. Long time behavior when $\omega_b \cap \omega_{c_+} = \emptyset$.
 $b = b_5(x) = \mathbf{1}_{[0.4,0.6]}(x)$ and $c = c_4(x) = \mathbf{1}_{[0.1,0.2]}(x)$

REFERENCES

- [1] F. Alabau-Boussouira, Z. Wang, and L. Yu. A one-step optimal energy decay formula for indirectly nonlinearly damped hyperbolic systems coupled by velocities. *ESAIM Control Optim. Calc. Var.*, **23** (2) (2017), 721–749.
- [2] W. F. Ames. *Numerical methods for partial differential equations*. Computer Science and Scientific Computing. Academic Press, Inc., Boston, MA, third edition, 1992.
- [3] S. Gerbi, C. Kassem, A. Mortada and A. Wehbe. Exact controllability and stabilization of locally coupled wave equations : theoretical results. *ZAA, Z. Anal. Anwend.*, to appear.

- [4] C. Kassem, A. Mortada, L. Toufayli, and A. Wehbe. Local indirect stabilization of N-d system of two coupled wave equations under geometric conditions. *C. R. Math. Acad. Sci. Paris*, **357**(6) (2019), 494–512.
- [5] K. Liu, Locally distributed control and damping for the conservative systems, *SIAM J. Control Optim.*, **35** (1997), 1574–1590.
- [6] C. Bardos, G. Lebeau and J. Rauch, Sharp sufficient conditions for the observation, control, and stabilization of waves from the boundary, *SIAM J. Control Optim.*, **30** (1992), 1024–1065.

LABORATOIRE DE MATHÉMATIQUES UMR 5127 CNRS & UNIVERSITÉ DE SAVOIE MONT BLANC, CAMPUS SCIENTIFIQUE, 73376 LE BOURGET DU LAC CEDEX, FRANCE
Email address: `stephane.gerbi@univ-smb.fr`

UNIVERSITÉ LIBANAISE, EDST, EQUIPE EDP-AN, HADATH, BEIRUT, LEBANON
Email address: `shiraz.kassem@hotmail.com`

UNIVERSITÉ LIBANAISE, EDST, EQUIPE EDP-AN, HADATH, BEIRUT, LEBANON
Email address: `amina_mortada2010@hotmail.com`

UNIVERSITÉ LIBANAISE, FACULTÉ DES SCIENCES 1, EDST, EQUIPE EDP-AN, HADATH, BEIRUT, LEBANON
Email address: `ali.wehbe@ul.edu.lb`